GLIA

GLIA 59:615–626 (2011)

Inducible Gene Expression in GFAP+ Progenitor Cells of the SGZ and the Dorsal Wall of the SVZ—A Novel Tool to Manipulate and Trace Adult Neurogenesis

TILLMANN WEBER,[1,2,3] VERA BAIER,[1] RAHEL PAULY,[1] AMAR SAHAY,[4] MAX BAUR,[1] ELKE HERRMANN,[1] FRANCESCA CICCOLINI,[5] RENÉ HEN,[4] GOLO KRONENBERG,[6,7] AND DUSAN BARTSCH[1]*

[1]*Department of Molecular Biology, Central Institute of Mental Health, Heidelberg University, Medical Faculty Mannheim, Mannheim, Germany*
[2]*Department of Addictive Behavior and Addiction Medicine, Central Institute of Mental Health, Heidelberg University, Mannheim, Germany*
[3]*Department of Psychiatry and Psychotherapy, Central Institute of Mental Health, Heidelberg University, Mannheim, Germany*
[4]*Division of Integrative Neuroscience, Department of Psychiatry, Columbia University, Kolb Annex, New York, New York*
[5]*Department of Neurobiology (IZN), Heidelberg University, Heidelberg, Germany*
[6]*Department of Neurology, Charité University Hospital, Charitéplatz, Berlin, Germany*
[7]*Department of Psychiatry and Psychotherapy, Charité-CBF, Eschenallee, Berlin, Germany*

KEY WORDS
neurogenesis; GFAP; astrocytes; radial glia; tTA; tet system; DTA

ABSTRACT
In the adult mammalian brain, neurogenesis originates from astrocyte-like stem cells. We generated a transgenic mouse line in which the tetracycline dependent transactivator (tTA) is expressed under the control of the murine GFAP promoter. In this mouse line, inducible gene expression targets virtually all GFAP-expressing stem-like cells in the dentate gyrus and a subset of GFAP-expressing progenitors located primarily in the dorsal wall/dorsolateral corner of the subventricular zone. Outside the neurogenic zones, astrocytes are infrequently targeted. We introduce a panel of transgenic mice which allow both inducible expression of candidate genes under control of the murine GFAP promoter and, at the same time, lineage tracing of all cells descendant from the original GFAP-positive cell. This new mouse line represents a versatile tool for functional analysis of neurogenesis and lineage tracing.

INTRODUCTION

In the adult mammalian brain, neurogenesis has been firmly established in two brain areas, the subventricular zone (SVZ), including the rostral migratory stream (RMS), and the hippocampal dentate gyrus (DG) (Doetsch, 2003; Gritti et al., 2002). Neural stem cells (NSC) with astrocytic characteristics including GFAP immunoreactivity are derived from radial glia and persist into adulthood in both the subgranular and subventricular zones (Alvarez-Buylla et al., 2002; Garcia et al., 2004; Merkle et al., 2004; Seri et al., 2001). In an elaborate, stepwise process involving several intermediate cell types, these NSCs mature into granule neurons in the hippocampal DG (Kempermann et al., 2004) or migrate through the RMS to the olfactory bulb (OB) where they form interneurons (Carleton et al., 2003).

In the past, the study of neurogenesis has relied on 3H-thymidine and BrdU-labeling. However, with the BrdU technique, a number of limitations such as toxicity (Taupin, 2007), nonproliferative DNA synthesis (Kuan et al., 2004) and difficulties in co-localizing nuclear BrdU staining with cell-type specific markers have to be taken into account (Kronenberg et al., 2003). Retrovirus-mediated lineage tracing may avoid these problems, but requires stereotactic injection of the virus into the brain, so lesion effects on neurogenesis have to be considered.

Mouse genetic fate mapping of adult neurogenesis with reporter proteins represents a major advance in available methodology (Imayoshi et al., 2008; Lagace et al., 2007; Ninkovic et al., 2007; Young et al., 2010). Increasingly, conditional genetic mouse models using CreERT/loxP technology enable researchers to delete target genes in neural precursors (Balordi and Fishell, 2007; Breunig et al., 2007; Colak et al., 2008; Kuo et al., 2006) and a number of studies have coupled this with lineage tracing (Gao et al., 2009; Lagace et al., 2008). By contrast, only few studies have described conditional tet-regulated overexpression of target genes in neural progenitors of adult mice (Dupret et al., 2008; Farioli-Vecchioli et al., 2008) and none have combined this with genetic fate mapping.

Here, we describe a conditional gene expression system that allows inducible expression of a candidate gene

Additional Supporting Information may be found in the online version of this article.

Tillmann Weber and Vera Baier contributed equally to this work.

Grant sponsor: German Research foundation (DFG); Grant number: SFB 636; Grant sponsor: The German Federal Ministry of Education and Research; Grant number: PNS-01GS08152-7 (NGFN-plus); Grant sponsor: The European Union; Grant number: MRTN-CT-2006-035367 (CAVNET) and HEALTH-F2-2007-201714 (DEVANX); Grant sponsor: Federal State Baden-Württemberg (collaborative Grant "Network Aging Research").

*Correspondence to: Dusan Bartsch, Department of Molecular Biology, Central Institute of Mental Health, University of Heidelberg, J5, Mannheim 68159, Germany. E-mail: dusan.bartsch@zi-mannheim.de

Received 2 July 2010; Accepted 25 November 2010

DOI 10.1002/glia.21129

Published online 3 February 2011 in Wiley Online Library (wileyonlinelibrary.com)

in GFAP+ neural progenitors and, at the same time, lineage tracing with the reporter protein β-galactosidase (βgal). We demonstrate the practicality and versatility of this approach with a panel of transgenic mice. First, we establish that transgenic mGFAP-tTA/Ptet-nLacZ and mGFAP-tTA/Ptet-EGFP mice target inducible gene expression to virtually all GFAP+ progenitor cells in the DG and to a subset of GFAP+ progenitors in the dorsal wall/dorsolateral corner of the SVZ. By contrast, the majority of GFAP+ astrocytes outside the neurogenic niches are not labeled. Next, we demonstrate that inducible labeling of GFAP+ progenitor cells with βgal allows tracing of adult neurogenesis in triple-transgenic mGFAP-tTA/Ptet-Cre/R26R mice. Finally, we describe quadruple-transgenic mGFAP-tTA/Ptet-DTA/Ptet-Cre/R26R mice that combine inducible gene expression of diphtheria toxin A (DTA) in GFAP+ progenitors of the DG with fate mapping of the entire process of adult neurogenesis with βgal. The dual system introduced here allows the study of both early and late developmental effects of gene overexpression in adult neural progenitor cells of the subgranular zone (SGZ) and the dorsal/dorsolateral wall of the SVZ.

MATERIALS AND METHODS

Generation of Transgenic Mice

To generate tet-promoter controlled diphtheria toxin A mice Tg(tetO-D/DTA) (Ptet-DTA), a cDNA encoding the debilitated diphtheria toxin A gene (D-DTA) (Maxwell et al., 1987) (generous gift of Joseph A. Gogos) was flanked by EcoRV sites by PCR and cloned into the EcoRV site of plasmid MM400 (Mayford et al., 1996). Seven Ptet-DTA transgenic founder mice were obtained by DNA microinjection with a NotI Ptet-DTA linearized fragment. Founders were functionally characterized by crossing them with a nestin-tTA transgenic mouse line (Sahay and Hen, unpublished observation). Ptet-DTA line 2.11 was used for all further studies.

To generate tet-promoter controlled EGFP mice Tg(tetO-EGFP) (Ptet-EGFP), a pBI-EGFP vector (Clontech) was digested with AatII and SapI to release the Ptet-EGFP sequence from its plasmid backbone. Five Ptet-EGFP transgenic founder mice were obtained by DNA microinjection. Founders were functionally characterized by crossing them with mGFAP-tTA mice. Ptet-EGFP line 167-38 was used for all subsequent studies.

To generate murine GFAP-promoter controlled transactivator (tTA) mice Tg(mGFAP-tTA) (mGFAP-tTA), a cDNA encoding the synthetic transactivator gene (Urlinger et al., 2000) was cloned into the NotI site of the C3123 plasmid (generous gift of Lennart Mucke) downstream of a 2 kb fragment of the murine GFAP-promoter (mGFAP) (Johnson et al., 1995) and released from its backbone with SfiI. Transgenic mice were generated by DNA microinjection. Seven mGFAP-tTA founder mice were obtained. mGFAP-tTA mice were functionally characterized by crossing them to tet-promoter (Ptet) controlled βgal reporter mice Tg(tetNZL)2Bjd/J (Ptet-nLacZ) (Schönig and Bujard, 2003) yielding double-transgenic mGFAP-tTA/Ptet-nLacZ mice. The mGFAP-tTA line 64-27, which was used for all subsequent analyses, was further characterized by generating double-transgenic mGFAP-tTA/Ptet-DTA and mGFAP-tTA/Ptet-EGFP mice through crossings with Ptet-DTA mice and Ptet-EGFP mice, respectively.

To characterize the fate-mapping capacity of the mGFAP-tTA line, we first created double-transgenic Ptet-Cre/R26R mice by mating B6;129S4-Gt(ROSA)26-Sor^{tm1Sor}/J mice (R26R) (Soriano, 1999) with B6;C-Tg(tetO-cre)LC1Bjd/BjdIbcm (Ptet-Cre) mice (Schönig et al., 2002). For the purpose of generating triple and quadruple transgenic mice, Ptet-Cre/R26R mice were bred to homozygosity. Homozygous Ptet-Cre/R26R mice were then either crossed to mGFAP-tTA mice to generate triple-transgenic mGFAP-tTA/Ptet-Cre/R26R mice or crossed to mGFAP-tTA/Ptet-DTA mice to obtain quadruple-transgenic mGFAP-tTA/Ptet-DTA/Ptet-Cre/R26R mice. Compared to matings with heterozygous Ptet-Cre/R26R mice the ratio of triple-transgenic mGFAP-tTA/Ptet-Cre/R26R and quadruple-transgenic mGFAP-tTA/Ptet-DTA/Ptet-Cre/R26R offspring from matings with homozygous Ptet-Cre/R26R mice increases from 1:8 to 1:2 and from 1:16 to 1:4, respectively.

Mice were housed individually and kept under a 12 h/12 h light/dark cycle with *ad libitum* access to food and water. All experimental procedures conformed to institutional guidelines and were approved by an official committee.

Doxycycline Treatment

Doxycycline (Dox) was given via drinking water sweetened with 5% sucrose. During matings and pregnancy 5 μg/mL Dox was given to inhibit binding of tTA to Ptet (referred to as "suppression"). Postnatally, the concentration of Dox was increased to 50 μg/mL to sustain effective transcriptional suppression. Ptet-controlled target gene expression was initiated by removing Dox from the drinking water (referred to as "activation").

Histological Procedures

Brains were perfusion-fixed with 4% paraformaldehyde and cut into 40-μm sections. For X-gal histochemistry, 5-bromo-4-chloro-3-indolyl-β-D-galactopyranoside (X-Gal; Sigma-Aldrich) was dissolved in dimethylformamide (20 mg/mL) (Sigma-Aldrich) and further diluted in staining solution consisting of 5 mM potassium ferricyanide, 5 mM potassium ferrocyanide, and 2 mM magnesium chloride in PBS to a final concentration of 1 mg X-Gal/mL staining solution. Antibodies were diluted in PBS containing 0.1% Triton X-100 and 10% normal donkey serum. The following primary antibodies were used: mouse α-GFAP (Sigma, 1:2,000), rabbit α-Ki67 (Abcam, 1:200), mouse α-NeuN (Chemicon, 1:4,000), goat α-Doublecortin (Santa Cruz, 1:500), rat α-Nestin (BD, 1:100), rabbit α-Sox2 (Chemicon, 1:1,000), chicken α-βgalactosidase

(Abcam, 1:10,000), mouse α-Calbindin (Swant, 1:2,000), rabbit α-Calretinin (Swant, 1:2,000), rabbit α-GFP (Invitrogen, 1:1,000), mouse α-tyrosine hydroxylase (Millipore, 1:500), mouse α-Parvalbumin (Sigma, 1:2,000), and mouse α-GAD67 (Chemicon, 1:500). Secondary antibodies conjugated to AF488 (Invitrogen), and to Cy2, Cy3, and Cy5 (Jackson ImmunoResearch) were used. Hoechst 33258 was used at a concentration of 0.5 μg/mL.

Quantification and Imaging

All confocal microscopy was performed using a Nikon A1R-CLEM confocal laser-scanning microscope (Nikon Imaging Center, BioQuant, Heidelberg, Germany). Appropriate gain and black level settings were determined on control tissues stained with secondary antibodies alone.

The number of ßgal+ cells in the DG was determined with a modified version of the fractionator principle essentially as described in earlier studies (Kempermann et al., 2003; Kronenberg et al., 2003). Briefly, ßgal+ cells were counted in every sixth sagittal brain section throughout the lateromedial extent of the granule cell layer (n = 3–4 mice per time point). The absolute number of ßgal+ cells was then estimated by multiplying the resulting counts by six, because every sixth section had been used. To avoid oversampling, cells that were in focus at the uppermost focal plane, when focusing into the section, were disregarded.

For phenotypic analyses of all antibody combinations of interest, 50–150 cells per mouse in the dentate gyrus (n = 3–4 mice per time point) were examined with immunofluorescent double and triple labeling and confocal microscopy. The absolute number of cells of a given phenotype was then derived by multiplying the absolute number of cells of the reference phenotype by the percentage of the phenotype of interest.

The number of ßgal+ cells per OB glomerulus was quantified as described in detail previously (Lagace et al., 2007). In short, 50 glomeruli per animal within three matched serial sections were analyzed (n = 3–4 mice per time point). The number of cells per glomerulus and the number of ßgal+ cells per glomerulus were counted.

In the GCL of the OB, the number of βgal+ cells was quantified in three matched serial sections per animal (n = 3–4 mice per time point). The GCL was subdivided into four reference areas (apical, central, dorsolateral, ventrolateral) of 300 μm^2 each. The number of ßgal+, NeuN+, and NeuN+/ßgal+ cells within these reference areas was quantified. Finally, the ratio of NeuN+/ßgal+ cells to all ßgal+ cells and to all NeuN+ cells within the reference space was calculated.

Statistical Analyses

The data are presented as mean ± SEM. Statistical analyses were performed using a one-way ANOVA followed by a Tukey *post hoc* test. All statistical analyses were performed using either SPSS (Chicago, IL; version 11.0.2) or Prism (version 5.0) software. $P < 0.05$ was considered statistically significant and $P < 0.001$ was considered highly significant.

RESULTS

The Murine GFAP Promoter Directs Transactivator Expression to GFAP+ Astrocytes in Regions of Adult Neurogenesis

Regulatory sequences (15 kb) of the murine GFAP gene were reported to drive transcription to adult GFAP-expressing neural stem cells (NSC), the predominant NSCs isolated from postnatal and adult forebrain (Garcia et al., 2004; Imura et al., 2003). In this study, a 2 kb murine GFAP (mGFAP) promoter fragment (Johnson et al., 1995) was used to control spatial expression of an improved version of the tetracycline-controlled transactivator protein (tTA) (Urlinger et al., 2000). In the absence of Dox, tTA binds to and activates promoters harboring tet-operator (tetO) sequences (Ptet) (Kistner et al., 1996).

First, we analyzed temporo-spatial regulation of functional tTA expression using double-transgenic mGFAP-tTA/Ptet-nLacZ mice (Fig. 1a) expressing Ptet-controlled, nuclear localized, reporter protein βgal (Schönig and Bujard, 2003). In mGFAP-tTA/Ptet-nLacZ mice, cells with ßgal activity (X-Gal+) were prominent in the dorsal aspect of the SVZ (Fig. 1c), RMS (Fig. 1b,c), and SGZ of the DG (Fig. 1d). In the SGZ, βgal+ cells displayed GFAP immunoreactivity along with a radial glia-like morphology with a single horizontal or apical process, respectively (Fig. 1e). Whereas βgal+/GFAP+ cells outside the neurogenic zones were rare and did not show remarkable proliferative activity as assessed by co-expression with cell cycle-associated marker Ki67 (lack of Ki67 immunoreactivity in 300 randomly selected βgal+/GFAP+ cells from three animals), some of the βgal+/GFAP+ astrocytes in SGZ and SVZ/RMS consistently showed Ki67 co-labeling (Fig. 1f,i,k,m), albeit at a very low percentage of the total cell population. In the SGZ, 1.9% of βgal+/GFAP+ cells showed Ki67 immunoreactivity while 2.2% in the SVZ and 3% in the RMS showed Ki67 colabeling (of 300 βgal+/GFAP+ cells in SGZ and SVZ and of 500 βgal+/GFAP+ cells in the RMS, respectively; analysis of three animals). βgal+/GFAP+/Ki67+ cells in the RMS (Fig. 1k,m) may represent resident progenitors that have previously been shown to actively contribute to OB neurogenesis (Alonso et al., 2008; Mendoza-Torreblanca et al., 2008; Merkle et al., 2007). DCX immunoreactivity was observed in a small fraction of βgal+ cells in the SGZ and SVZ/RMS (<1% of βgal+ cells, respectively; analysis of 300 cells from three different animals per brain region) (Fig. 1g,j,l,n). Furthermore, βgal+ cells consistently lacked NeuN immunoreactivity in DG and OB (Fig. 1h,n).

We also studied functional mGFAP-tTA controlled gene expression using Ptet-EGFP mice as a second reporter line (Fig. 1o). Analysis of double-transgenic mGFAP-tTA/Ptet-EGFP mice confirmed reporter protein

expression in GFAP+ cells of SGZ, dorsal aspect of the SVZ and RMS (Fig. 1p–r), thereby recapitulating the βgal expression pattern of mGFAP-tTA/Ptet-nLacZ mice.

Taken together, the 2 kb fragment of the murine GFAP promoter reliably directs tTA expression to GFAP+ cells in the SGZ, SVZ, and RMS which allows inducible Ptet-controlled candidate gene overexpression in these regions.

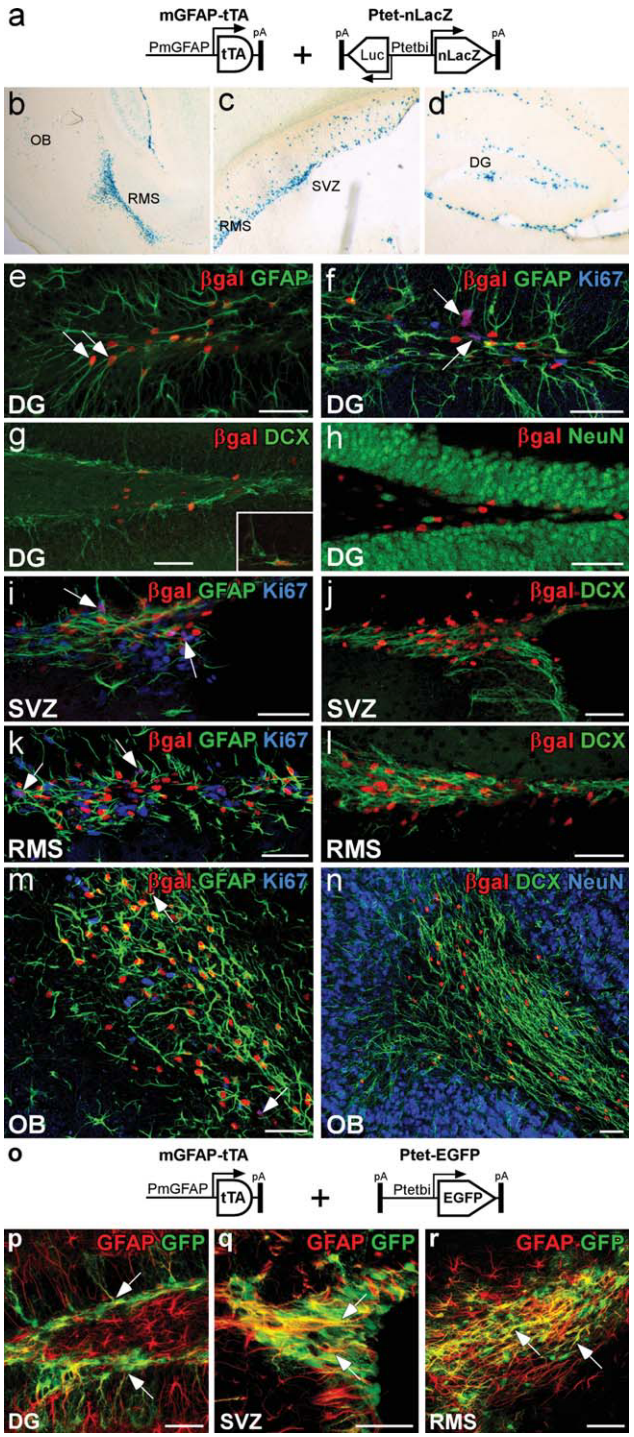

Expression of tTA in GFAP+ Astrocytes of the SGZ and Dorsal Wall/Dorsolateral Corner of the SVZ Allows Fate Mapping of Adult Neurogenesis

We generated triple-transgenic mGFAP-tTA/Ptet-Cre/R26R mice (Fig. 2a) in which mGFAP-tTA controls inducible expression of Ptet-Cre (Schönig et al., 2002). In the absence of Dox, Cre expression results in the removal of a loxP-flanked stop-cassette in the Rosa26 locus (R26R), thus allowing cytosolic expression of βgal under the control of the ubiquitously active Rosa26 promoter (Soriano, 1999).

Dox was administered in the drinking water during embryogenesis and postnatally until P21. Brains of mice analyzed under Dox suppression did not show X-Gal staining. Mice were then activated by discontinuation of Dox at P21 and analyzed 12 weeks later. The overall X-Gal staining pattern in mGFAP-tTA/Ptet-Cre/R26R mice (Fig. 2b–d) was largely similar to that observed in mGFAP-tTA/Ptet-nLacZ mice (see Fig. 1b–d). However, mGFAP-tTA/Ptet-Cre/R26R mice showed additional X-Gal staining in the granule cell layer (GCL) and glomerular layer (GL) of the OB (Fig. 2b) and in the granule cell layer of the DG (Fig. 2d). Phenotypic analyses of βgal-expressing cells in the adult neurogenic areas revealed reporter protein expression in all key developmental milestones of neurogenesis in the DG and SVZ/RMS/OB (Kempermann et al., 2004) (Fig. 2e–r). As expected, we found βgal expression in GFAP+ cells characterized by a radial glia-like morphology (Fig. 2e,j). These ßgal+ type-1 cells co-labeled with other type-1

Fig. 1. Double-transgenic mGFAP-tTA/Ptet-nLacZ and mGFAP-tTA/Ptet-EGFP reporter mice. (**a**) Illustration of transgenic mGFAP-tTA (transactivator line) and Ptet-nLacZ (tet-response line) mouse lines. In the transactivator line, a 2 kb murine GFAP promoter fragment (PmGFAP) controls tTA expression. In double-transgenic mGFAP-tTA/Ptet-nLacZ mice, tTA binds to the tet-promoter (Ptetbi) in the absence of Dox, thereby initiating expression of the Ptet-controlled reporter gene LacZ (Ptet-nLacZ). Ptet-controlled βgal expression in mGFAP-tTA/Ptet-nLacZ mice was suppressed with Dox until P21. Mice were then activated by discontinuation of Dox and analyzed 12 weeks later. (**b–d**) X-gal staining shows βgal activity in the SVZ/RMS (b,c) and in the hippocampus, including the DG (d) whereas no βgal expression is seen in the granular and glomerular cell layers of the OB (b). (**e–n**) Immunohistochemical analysis reveals a glial phenotype of βgal+ cells both in DG (e-h) as wells as in SVZ/RMS and OB (i-n). (e) βgal+ cells in the SGZ frequently show GFAP+ radial glia-like apical processes (arrows) characteristic of type-1 cells (Filippov et al., 2003; Kronenberg et al., 2003). (f) A small fraction of βgal+/GFAP+ cells show colabeling with interphase marker Ki67 (arrows). The low ratio of GFAP+/Ki67+/βgal+ to GFAP+/βgal+ cells suggests slow proliferative activity of these cells. (g) With few exceptions (inset), the majority of βgal+ cells in the SGZ lacks DCX immunoreactivity. (h) NeuN+/βgal+ neurons were never encountered in the DG. (i,k,m) βgal+ cells in the SVZ (i), RMS (k) and OB (m) show GFAP immunoreactivity. Again, these cells show low proliferative activity as indicated by rare Ki67 coexpression (arrows) (i,k,m). Furthermore, the majority of βgal+ cells in SVZ, RMS and OB do not show DCX immunoreactivity (j,l,n) and βgal+ cells consistently lacked NeuN expression (n). (**o**) Illustration of transgenic mGFAP-tTA and Ptet-EGFP mouse lines. Ptet-controlled EGFP expression in mGFAP-tTA/Ptet-EGFP mice was suppressed with Dox until P21. Mice were then activated by discontinuation of Dox and analyzed 12 weeks later. (**p–r**) Similar to mGFAP-tTA/Ptet-nLacZ mice, reporter protein expression (EGFP) is confined to GFAP+ cells in neurogenic areas of the DG (p, arrows), SVZ (q, arrows) and RMS (r, arrows). Scale bars in e–n, p–r: 50 μm.

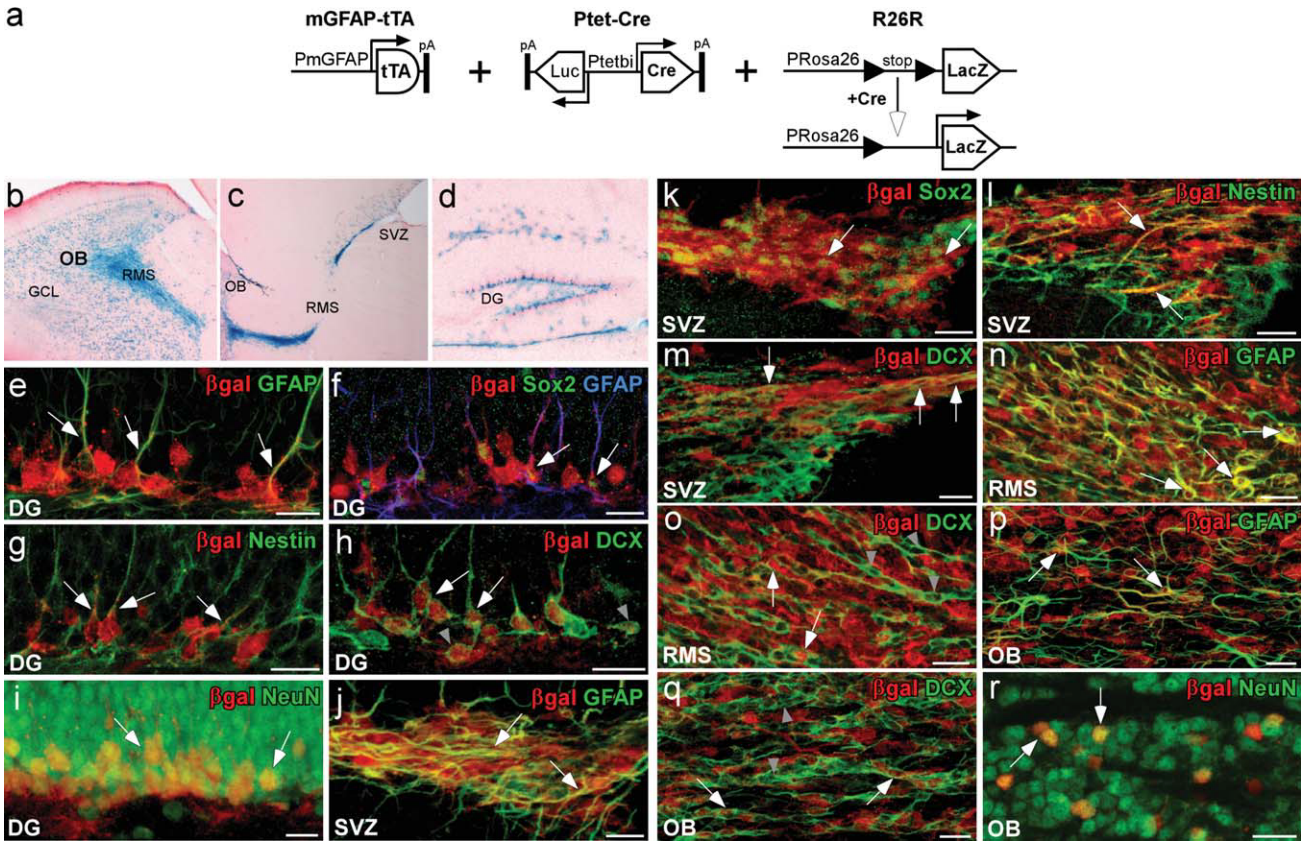

Fig. 2. Triple-transgenic mGFAP-tTA/Ptet-Cre/R26R mice allow fate-mapping of adult neurogenesis. (**a**) Triple-transgenic mGFAP-tTA/Ptet-Cre/R26R mice were generated by crossing mGFAP-tTA mice with double-transgenic Ptet-Cre/R26R mice which are homozygous for both transgenes. In the absence of Dox, tTA binding to the tet-promoter (Ptetbi) activates Cre expression (Ptet-Cre), which in turn deletes a loxP flanked stop cassette in the ubiquitously active Rosa26 locus (R26R), thereby initiating constitutive βgal expression. Induction of βgal expression in mGFAP-tTA/Ptet-Cre/R26R mice was suppressed with Dox until P21. Mice were then activated by discontinuation of Dox and analyzed 12 weeks later. (**b–d**) X-Gal staining reveals βgal expression in the dorsal aspect of the lateral ventricle (c) RMS (b,c) and DG (d). In contrast to mGFAP-tTA/Ptet-nLacZ mice (Fig. 1b) and mGFAP-tTA/Ptet-EGFP mice (Supp. Info. Fig. 3d), X-Gal staining can now be recognized throughout the granular and glomerular layer of the OB (b) and in the GCL of the DG (d). (d) Intense X-Gal staining in the DG is localized to both the SGZ and the GCL. (**e–r**) Immunohistochemical analysis of mGFAP-tTA/Ptet-Cre/R26R mice confirms targeting of GFAP+ progenitors and subsequent fate mapping of the major developmental steps of adult neurogenesis. (e–g) βgal expression by radial glia-like stem cells (type-1 cells) in the SGZ. βgal+ cells with characteristic apical processes extending through the GCL arrows show colabeling with GFAP (e), Sox2 (f) and nestin (g). (h) βgal+/DCX+ cells in the SGZ show short tangential processes resembling type-2b transit amplifying cells (arrowheads) or type-3 neuroblasts (arrows) (Kempermann et al., 2004). (i) Newly generated βgal+/NeuN+ neurons reside in the GCL of the DG (arrows). (j-l) Analysis of βgal+ cells in the SVZ reveals colabeling with GFAP (j, arrows), Sox2 (k, arrows) and nestin (l, arrows). (m) βgal+/DCX+ cells in the SVZ are located in the dorsal/dorsolateral wall of the lateral ventricle (arrows). (n,o) In the RMS (rostral part), βgal+ cells frequently show GFAP immunoreactivity (n, arrows). Both DCX+/βgal+ (arrows) and DCX+/βgal-negative (arrowheads) neuroblasts migrate through the RMS toward the OB (o). (p-r) βgal staining in the OB. Again, local GFAP+ cells show co-labeling with βgal (p, arrows). (q) Both DCX+/βgal+ cells (arrows) and DCX+/βgal negative cells (arrowheads) migrate toward their destination in the OB. (r) Newly generated NeuN+/βgal+ neurons (arrows) reside in the GCL of the OB. Scale bars in e-r: 20 μm.

cell markers like Sox2 and nestin (Fig. 2f,g,k,l). In contrast to double-transgenic mGFAP-tTA/Ptet-nLacZ and mGFAP-tTA/Ptet-EGFP mice, ßgal immunoreactivity was also detected in the progeny of GFAP+ type-1 cells, namely in DCX+ transit-amplifying cells (type-2b) (Fig. 2h), DCX+ neuroblasts (Fig. 2h,m,o,q), and mature NeuN+ neurons (Fig. 2i,r). Importantly, neurons outside the neurogenic areas consistently lacked βgal immunoreactivity.

Next, the kinetics of fate mapping in the DG of mGFAP-tTA/Ptet-Cre/R26R mice were analyzed at 2, 4, and 12 weeks after Dox withdrawal using immunohistochemistry (Fig. 3a–d; Supp. Info. Fig. 1a–i). At 2 weeks, only few βgal+ cells were detected in the DG (Fig. 3b; Supp. Info. Fig. 1a–c). Approximately two-thirds of these βgal+ cells were GFAP+ (Fig. 3a; Supp. Info. Fig. 1a) and showed type-1 cell morphology (Fig. 3c; Supp. Info. Fig. 1a). Additionally, approximately one-third of βgal+ cells were DCX+ (Fig. 3a; Supp. Info. Fig. 1b). By contrast, we did not detect NeuN+/βgal+ neurons at 2 weeks after Dox withdrawal (Fig. 3a,d; Supp. Info. Fig. 1c). After 4 weeks of activation, the number of βgal+ cells in the DG had increased significantly (Fig. 3b; Supp. Info. Fig. 1d–f). This increase was accompanied by a doubling of βgal+/GFAP+ type-1 cells (Fig. 3c). Also, the first newborn βgal+/NeuN+ neurons emerged in the GCL at 4 weeks after Dox withdrawal (Fig. 3a,d; Supp. Info. Fig. 1f). Finally, after 12 weeks of activation, the significant further increase in βgal+ cells in the DG (Fig. 3b; Supp. Info. Fig 1g–i) was mainly attributable to an accu-

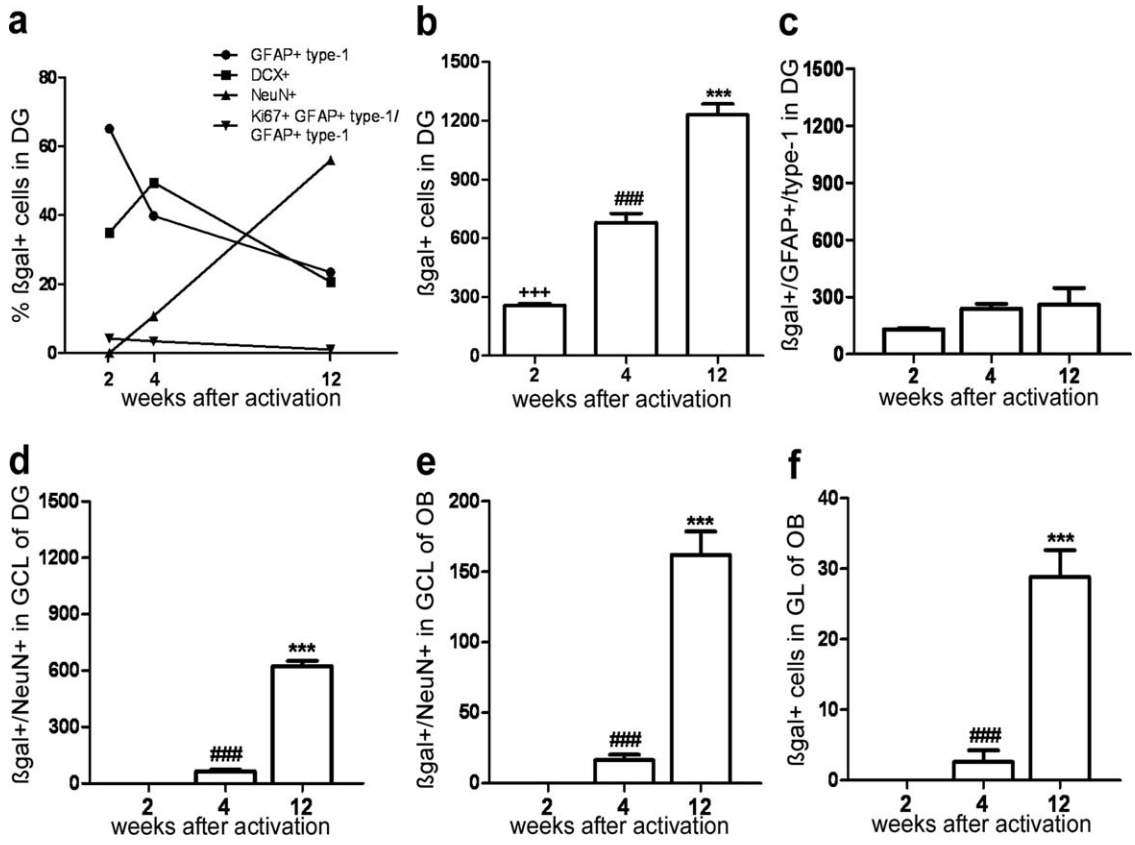

Fig. 3. Quantitative fate mapping of neurogenesis in triple-transgenic mGFAP-tTA/Ptet-Cre/R26R mice. Triple-transgenic mGFAP-tTA/Ptet-Cre/R26R mice were sacrificed after 2, 4, and 12 weeks of activation, respectively (n = 3-4 mice per time point). (**a**–**d**) Analysis of hippocampal neurogenesis. (a) Phenotypic analysis of βgal-expressing cells (analysis of 50–150 cells per staining per animal). (b) Total number of βgal-expressing cells in DG. (c) Total number of βgal+/GFAP+ type-1 cells in the SGZ. (d) Total number of βgal+/NeuN+ neurons in GCL of DG. (**e**,**f**) Analysis of neurogenesis in the olfactory bulb. (e) GCL of OB. (f) GL of OB. For details regarding quantification, please refer to Materials and Methods. $^{+++}P < 0.001$, 2 weeks versus 4 weeks; $^{\#\#\#}P < 0.001$, 4 weeks versus 12 weeks; $^{***}P < 0.001$, 2 weeks versus 12 weeks.

mulation of newborn βgal+/NeuN+ neurons in the GCL of the DG (56% of all βgal+ cells) (Fig. 3a,d; Supp. Info. Fig. 1i). By contrast, the number of βgal+/GFAP+/type-1 cells did not show a further increase between 4 and 12 weeks of activation (Fig. 3c; Supp. Info. Fig. 1g).

Then we analyzed the kinetics of reporter protein activation in the SVZ/RMS/OB of mGFAP-tTA/Ptet-Cre/R26R mice (Fig. 3e–f; Supp. Info. Fig. 2a–i). After 2 weeks of activation, only few βgal+ cells in the dorsal aspect of the SVZ could be identified (Supp. Info. Fig. 2a,b). Most of these cells in the SVZ were βgal+/GFAP+ (Supp. Info. Fig. 2a) while NeuN+/βgal+ neurons in the OB could not be detected at this early time point after induction of Ptet-controlled gene expression (Fig. 3e,f; Supp. Info. Fig. 2g). After 4 weeks, and even more so after 12 weeks, both the number of βgal+/GFAP+ cells and the number of βgal+/DCX+ cells had increased in the dorsal SVZ (Supp. Info. Fig. 2c–f). After 4 weeks of activation, the first newborn mature βgal+/NeuN+ neurons were detected in the GCL and GL of the OB (Fig. 3e,f; Supp. Info. Fig. 2h). The number of βgal+/NeuN+ neurons showed a further increase after 12 weeks of activation (Fig. 3e,f; Supp. Info. Fig. 2i; Fig. 4a,b).

Specifically, after 12 weeks of activation, 4.9% of NeuN+ neurons located in the GCL showed βgal immunoreactivity. βgal+ cells in the GCL were consistently GAD67 immunoreactive (analysis of 300 cells from three different animals) confirming GABAergic neuronal differentiation (Kohwi et al., 2007) (Fig. 4c). Eighty-one percent of βgal+ cells in the GCL expressed mature neuronal marker NeuN which is in line with ongoing differentiation of βgal+ cells and their progeny into mature postmitotic neurons (analysis of 300 βgal+ cells from 3 different animals). In the glomerular layer (GL), 2.6% of all GL neurons showed βgal immunoreactivity. 76% of these βgal+/NeuN+ cells co-labeled with GABAergic marker GAD67 (Fig. 4d). Furthermore, 33% of βgal+ cells in the GL showed Calretinin immunoreactivity (Fig. 4e), while 10% showed tyrosine hydroxylase (TH) co-labeling (Fig. 4f). Consistent with the adult origin of Calbindin+ neurons from the lateral wall of the SVZ (Merkle et al., 2007), Calbindin+ neurons consistently lacked βgal immunoreactivity in our mGFAP-tTA/Ptet-Cre/R26R mice (analysis of 100 glomeruli from three different animals) (Fig. 4b,e). Similarly, Parvalbumin+ neurons in the external plexiform layer (EPL) lacked βgal (analysis of 100

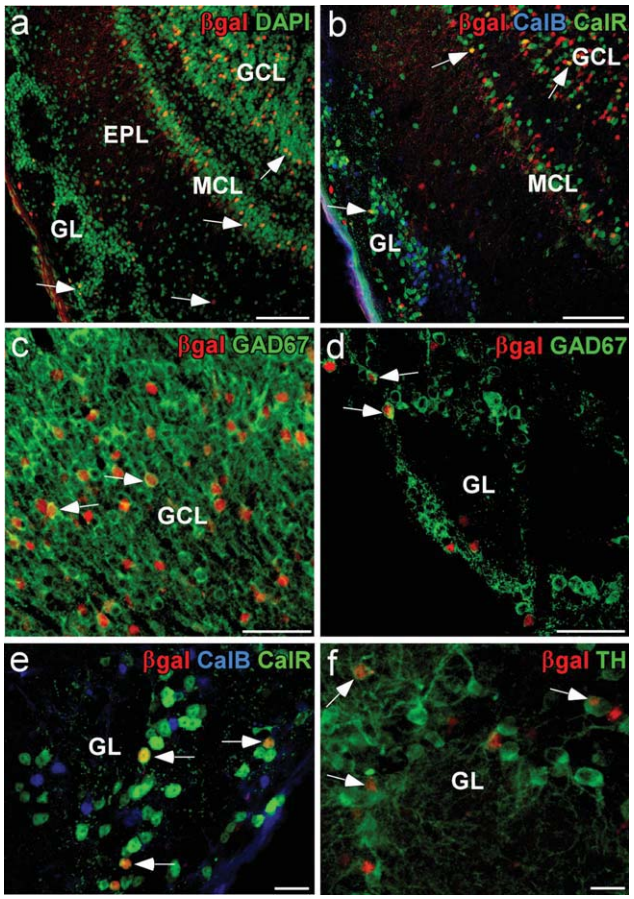

Fig. 4. Contribution of GFAP+/βgal+ progenitor cells to adult neurogenesis in the OB of mGFAP-tTA/Ptet-Cre/R26R mice. βgal expression was suppressed with Dox until P21. Mice were then activated by discontinuation of Dox and analyzed 12 weeks later. (**a**) βgal-expressing cells are widespread throughout all regions of the OB (arrows), including the glomerular layer (GL), external plexiform layer (EPL), mitral cell layer (MCL), and granule cell layer (GCL). (**b**) βgal+ cells in GL, MCL and GCL show Calretinin immunoreactivity (CalR; arrows), but lack Calbindin expression (CalB). (**c**,**d**) βgal+ neurons express GABAergic neuronal marker GAD67 in GCL (c, arrows) and GL (d, arrows). In the GL, βgal+ cells colabel with Calretinin (**e**, arrows) and tyrosine hydroxylase (TH) (f, arrows), but consistently lack Calbindin immunoreactivity (b,e). Scale bars in a,b: 100 μm, in c,d: 50 μm, in e,f: 20 μm.

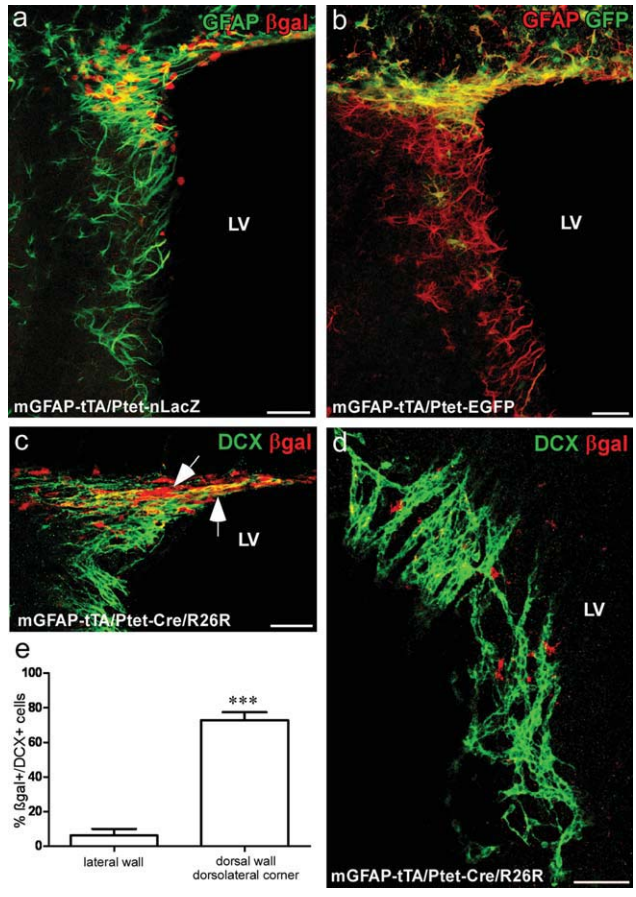

Fig. 5. Ptet-controlled gene expression is restricted to the dorsal wall/dorsolateral corner of the lateral ventricle in mGFAP-tTA mice. (**a**–**d**) Double- and triple-transgenic mice in which Ptet-controlled gene expression is spatially controlled by mGFAP-tTA were suppressed with Dox until P21. Mice were then activated by discontinuation of Dox and analyzed 12 weeks later. (a) In mGFAP-tTA/Ptet-nLacZ mice, βgal+/GFAP+ cells were primarily found in the dorsal wall/dorsolateral corner of the SVZ. (b) In mGFAP-tTA/Ptet-EGFP mice, GFP+/GFAP+ cells were similarly distributed. (c–**e**) Analysis of mGFAP-tTA/Ptet-Cre/R26R fate-mapping mice revealed that DCX+ cells coming from the dorsal wall/dorsolateral corner (c) of the SVZ typically show βgal expression (arrows) whereas the majority of DCX+ neuroblasts in the lateral wall (d) lack βgal immunoreactivity. ***$P < 0.001$. Scale bars in a–d: 50 μm.

Parvalbumin+ neurons from three different animals), which is in accordance with their generation during development (Young et al., 2007). Thus, βgal+/GFAP+ progenitor cells in the SVZ of mGFAP-tTA/Ptet-Cre/R26R mice give rise to GABAergic interneurons in the OB, including Calretinin+ and TH+ periglomerular neurons.

βgal+ cells in the SVZ of mGFAP-tTA/Ptet-Cre/R26R fate-mapping mice were primarily located in the dorsal wall/dorsolateral corner of the lateral ventricle whereas the lateral wall was hardly targeted (Fig. 5c,d). Similarly, βgal+ cells of mGFAP-tTA/Ptet-nLacZ mice and GFP+ cells of mGFAP-tTA/Ptet-EGFP mice were predominantly found in the dorsal aspect of the SVZ (Fig. 5a,b). In mGFAP-tTA/Ptet-Cre/R26R mice, at 12 weeks after Dox withdrawal, 75% of all GFAP+ cells in the dorsal wall/dorsolateral corner of the SVZ were βgal+ whereas only 19% of GFAP+ cells in the lateral wall were βgal+ (analysis of at least 300 GFAP+ cells each from 3 different animals). When βgal expression in DCX+ cells of the SVZ was analyzed in a region-specific manner, we found that 76% of all DCX+ immature neurons originating from the dorsal wall/dorsolateral corner of the lateral ventricle were ßgal+ (analysis of 300 DCX+ cells each from three different animals) (Fig. 5c,e). By contrast, only 8% of DCX+ cells coming from the lateral ventricle wall were ßgal+ (analysis of 300 DCX+ cells each from three different animals) (Fig. 5d,e). The restricted localization of GFAP+/βgal+ cells to the dorsal/dorsolateral SVZ with high numbers of DCX+/βgal negative cells leaving the lateral wall of the SVZ explains the high proportion of DCX+ cells lacking βgal (60%) in the RMS and OB (analysis of 300 DCX+ cells each from three different animals) (Fig. 2o,q).

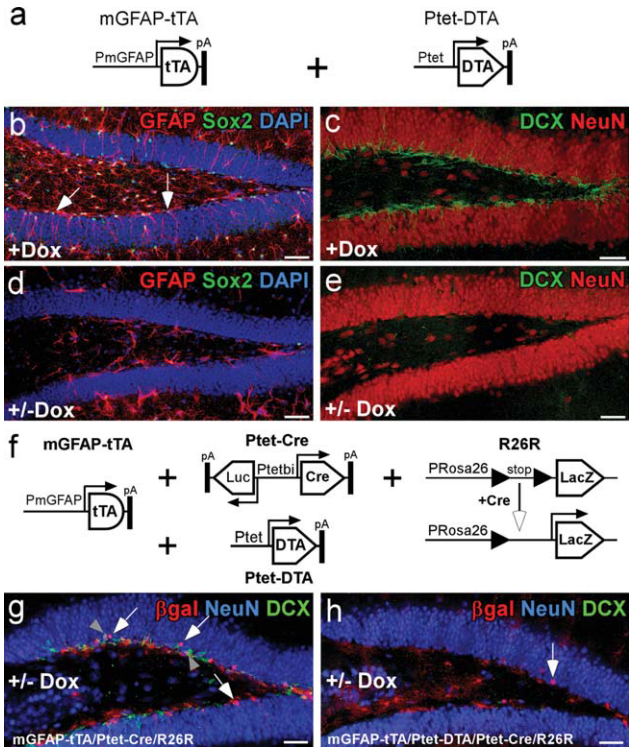

Fig. 6. Disruption of adult neurogenesis in the DG by targeted DTA expression in GFAP+ progenitor cells. (**a**) In double-transgenic mGFAP-tTA/Ptet-DTA mice, tTA binds to the tet-promoter (Ptet) in the absence of Dox, thereby initiating diphteria toxin A (DTA) gene expression. (**b–e**) Conditional DTA expression in GFAP+ cells of the DG leads to ablation of hippocampal neurogenesis. (b,c) In the presence of Dox which suppresses DTA expression (+Dox), mGFAP-tTA/Ptet-DTA mice show many GFAP+/Sox2+ cells in the SGZ (b, arrows) and abundant DCX immunoreactivity (c) in the DG. (d,e) By contrast, 12 weeks after DTA activation beginning at P21 (+/-Dox), the SGZ is devoid of GFAP+/Sox2+ cells (d) and DCX+ neuroblasts have disappeared from the DG (e). (**f**) mGFAP-tTA/Ptet-DTA mice were further crossed to double transgenic mice homozygous for both Ptet-Cre and R26R (Ptet-Cre/R26R) to generate quadruple-transgenic mGFAP-tTA/Ptet-DTA/Ptet-Cre/R26R mice. In the absence of Dox, mGFAP-promoter (PmGFAP) driven tTA expression (mGFAP-tTA transgene) leads to simultaneous tet-promoter (Ptetbi and Ptet) controlled gene expression of Cre recombinase (Ptet-Cre) and DTA (Ptet-DTA). Through recombination, Cre then initiates constitutive βgal expression (R26R) which is independent of continuous mGFAP-promoter activity, thus allowing fate mapping. (**g**,**h**) Fate mapping of DTA expression in GFAP+ progenitor cells confirms disruption of adult neurogenesis in the DG of mGFAP-tTA/Ptet-DTA/Ptet-Cre/R26R mice. At P21, mGFAP-tTA/Ptet-Cre/R26R control mice (g) and mGFAP-tTA/Ptet-DTA/Ptet-Cre/R26R mice (h) were activated by Dox withdrawal for 12 weeks. (g) In the DG of mGFAP-tTA/Ptet-Cre/R26R control mice, regular adult neurogenesis can be appreciated with a large number of βgal+ cells in the SGZ, DCX+ neuroblasts (arrowheads) and newborn βgal+/NeuN+ neurons in the GCL (arrows). (h) By contrast, mGFAP-tTA/Ptet-DTA/Ptet-Cre/R26R mice show only sparse βgal staining in the SGZ, a loss of most DCX+/βgal+ neuroblasts and only solitary newborn βgal+/NeuN+ neurons (arrow). Scale bars in b–e, g–h: 50 μm.

mGFAP-tTA Mice Predominantly Target GFAP+ Progenitor Cells in the Neurogenic Zones of the Adult Mouse Brain

Ptet-controlled reporter protein (βgal and EGFP) expression was analyzed through the rostrocaudal extent of the brain outside the neurogenic niches using both mGFAP-tTA/Ptet-nLacZ and mGFAP-tTA/Ptet-EGFP mice. Animals were suppressed with Dox until P21 and then activated without Dox for 12 weeks (+/− Dox). Outside the adult neurogenic zones, reporter protein expression in both lines was confined to GFAP+ astrocytes with most brain regions virtually devoid of transgene expression (Supp. Info. Fig. 3). Ptet-controlled expression of βgal and EGFP was identified in the fimbria of hippocampus (fi), the entire hippocampus (HC) (specifically the polymorphic layer and along the hippocampal fissure), the corpus callosum (cc) and the white matter of the cerebellum (CB) (Supp. Info. Fig. 3a–d) whereas Bergmann glia in the cerebellum was not targeted (Supp. Info. Fig. 3b,d). However, even in these brain regions, only a subset of GFAP+ astrocytes showed reporter protein expression (Supp. Info. Fig. 3e,f).

Furthermore, permanent βgal labeling in mGFAP-tTA/Ptet-Cre/R26R fate-mapping mice after 12 weeks of Dox withdrawal yielded βgal immunoreactivity in the same brain areas as in the double-transgenic reporter mice (Supp. Info. Fig. 3g). Specifically, X-Gal staining of GFAP+ astrocytes in non-neurogenic brain regions was similar to the staining pattern observed in Ptet-controlled reporter mice. Note that Bergmann glia was also not targeted in mGFAP-tTA/Ptet-Cre/R26R mice if the animals had been suppressed with Dox until P21 (Supp. Info. Fig. 3g,h). However, we found intense X-Gal staining of Bergmann glia when Ptet-controlled gene expression had been permanently activated without Dox (Supp. Info. Fig. 3i).

In conclusion, only a subset of GFAP+ astrocytes in distinct brain regions is targeted in mGFAP-tTA mice making this line relatively selective for GFAP+ progenitor cells in the SGZ and dorsal SVZ while sparing the majority of astrocytes in the rest of the brain.

Expression of Diphtheria Toxin A (DTA) in GFAP+ Astrocytes of the SGZ Disrupts Hippocampal Neurogenesis

Next, we generated double-transgenic GFAP-tTA/Ptet-DTA mice (Fig. 6a). DTA expression leads to cell death through inhibition of RNA translation (Yamaizumi et al., 1978). Unlike thymidine kinase's mode of action, which requires ganciclovir to kill dividing cells (Delaney et al., 1996; Garcia et al., 2004), cytotoxicity of DTA is independent of the cell cycle. Hence, this genetic system is particularly well suited to ablate the radial glia-like GFAP+ cells in the SGZ which have been previously reported to divide only rarely (Kronenberg et al., 2003). Again, Dox was administered until P21 in mGFAP-tTA/Ptet-DTA mice. DTA expression was then activated for 12 weeks in the absence of Dox when mice were sacrificed for histological analysis.

Twelve weeks after Dox withdrawal (+/- Dox mice), the density of GFAP+ cells in the hippocampus of activated mGFAP-tTA/Ptet-DTA mice was moderately reduced (Supp. Info. Fig. 4b) and changes in astrocyte morphology such as enlarged cell bodies and swollen processes were apparent (Supp. Info. Fig. 4b; Fig. 6d). The reduction in astrocyte numbers was most prominent in the polymorphic layer of the DG (Supp. Info. Fig. 4b;

Fig. 6d). Importantly, the SGZ was virtually devoid of radial glia-like GFAP+/Sox2+ cells (reduction by 95%) (Fig. 6d). Correspondingly, the number of DCX+ neuroblasts (Fig. 6e) in the DG was also reduced by more than 90% demonstrating efficient ablation of hippocampal neurogenesis by eliminating GFAP+ type-1 cells in the SGZ (comparisons of three age-matched, chronically Dox-suppressed double-transgenic mGFAP-tTA/Ptet-DTA mice with three mGFAP-tTA/Ptet-DTA mice activated for 12 weeks after discontinuation of Dox at P21).

In summary, targeting efficacy for GFAP+ type-1 cells in mGFAP-tTA/Ptet-DTA mice was close to 100% resulting in near-complete ablation of adult hippocampal neurogenesis.

Inducible DTA Overexpression in GFAP+ Progenitor Cells and Simultaneous Fate Mapping of Their Progeny in the DG of mGFAP-tTA/Ptet-DTA/Ptet-Cre/R26R Mice

Finally, we combined DTA expression in GFAP+ progenitor cells with visualization of their progeny using quadruple-transgenic mGFAP-tTA/Ptet-DTA/Ptet-Cre/R26R mice (Fig. 6f). For this purpose, mGFAP-tTA/Ptet-DTA mice were crossed with double-homozygous Ptet-Cre/R26R mice. Ptet-controlled gene expression was again suppressed with Dox until P21 followed by 12 weeks of activation in the absence of Dox. At this time, the number of βgal+ cells in the SGZ was greatly reduced. βgal+/DCX+ neuroblasts and βgal+/NeuN+ neurons could hardly be detected in the GCL of the DG compared with triple-transgenic mGFAP-tTA/Ptet-Cre/R26R control mice (Fig. 6g,h). Hence, combining Ptet-controlled gene overexpression in GFAP+ progenitor cells (mGFAP-tTA/Ptet-DTA) with fate-mapping (Ptet-Cre/R26R) not only allows cell-type specific, conditional overexpression of target genes but also subsequent βgal-tracing of the entire process of adult neurogenesis.

In contrast to the situation in the DG, analysis of the dorsal and lateral wall of the SVZ of activated mGFAP-tTA/Ptet-DTA mice did not show a reduction in the number of GFAP+ cells ($n = 3$; comparison to three age-matched, chronically Dox-suppressed double-transgenic mGFAP-tTA/Ptet-DTA mice) (Supp. Info. Fig. 4d). In mGFAP-tTA/Ptet-DTA/Ptet-Cre/R26R mice, we observed continuous βgal-labeling in GFAP+ progenitors (Supp. Info. Fig. 4f) and their DCX+ progeny in the dorsal wall of the lateral ventricle (Supp. Info. Fig. 4h) which confirms that Ptet-controlled DTA expression does not occur in GFAP+ progenitor cells of the SVZ. This result is somewhat in contrast to the findings described above regarding reliable and efficient Ptet-controlled targeting of candidate genes (Ptet-nlacZ, Ptet-EGFP, Ptet-Cre) to the dorsal wall/dorsolateral corner of the SVZ with mGFAP-tTA mice (Fig. 5a–c).

DISCUSSION

In this study, we describe an mGFAP-tTA mouse line which allows efficient, Ptet-controlled gene expression in virtually all astroglia-like stem cells located in the adult SGZ. In the SVZ, the mGFAP-tTA line region specifically targets inducible gene expression to GFAP+ progenitors of the dorsal wall/dorsolateral corner of the lateral ventricle while sparing its lateral wall. Outside the adult neurogenic zones, only a fraction of GFAP+ astrocytes in restricted brain areas is targeted making this line relatively selective for GFAP+ progenitor cells in the neurogenic zones of the adult brain. Finally, we describe a conditional gene expression system which allows inducible candidate gene expression in GFAP+ progenitor cells and, at the same time, lineage tracing of all cells descendent from the GFAP+ cell in which transgene expression had occurred. The dual system introduced here may serve as a versatile tool to study both early and late developmental effects of gene overexpression in adult neural progenitor cells of the SGZ and of the dorsal/dorsolateral wall of the SVZ.

The Murine GFAP Promoter Targets Inducible Ptet-Controlled Gene Expression to GFAP+ Progenitor Cells in the DG and in the Dorsal Wall/Dorsolateral Corner of the SVZ

GFAP+ cells are the principal source of adult forebrain neurogenesis (Garcia et al., 2004; Merkle et al., 2004; Seri et al., 2001). The full-length murine GFAP promoter (15 kb) has been utilized previously to direct Cre or thymidine-kinase (tk) expression to GFAP+ progenitors (Garcia et al., 2004; Gregorian et al., 2009). Here, we show that a 2 kb fragment of the murine GFAP promoter (Johnson et al., 1995) directs tTA expression (mGFAP-tTA), and consequently Ptet-controlled gene expression, to radial glia-like GFAP+ cells in mGFAP-tTA/Ptet-nLacZ and mGFAP-tTA/Ptet-EGFP mice. Taking advantage of triple-transgenic GFAP-tTA/Ptet-Cre/R26R mice which harbor the identical mGFAP-tTA transgene, but allow fate mapping using βgal as a reporter protein, we demonstrate that the entire process of adult hippocampal neurogenesis, including intermediate developmental stages, originates from these GFAP+/βgal+ cells in the SGZ. Ablation of GFAP+ progenitor cells in transgenic mGFAP-tTA/Ptet-DTA mice, which inducibly express DTA in GFAP+ cells, therefore, results in the complete disruption of adult neurogenesis in the dentate gyrus.

mGFAP-tTA mice also target GFAP+ astrocytes in the SVZ, which give rise to new neurons in the OB (Doetsch et al., 1999; Garcia et al., 2004). To our surprise, GFAP+/reporter protein+ astrocytes in mGFAP-tTA/Ptet-nLacZ and mGFAP-tTA/Ptet-EGFP mice were primarily located in the dorsal wall/dorsolateral corner of the lateral ventricles. Similarly, in mGFAP/Ptet-Cre/R26R mice used for lineage tracing, GFAP+/βgal+ cells were most prominent in the dorsal wall/dorsolateral corner of the lateral ventricles and largely absent from the lateral wall. In line with this observation, DCX+ neuroblasts migrating from the lateral ventricle wall were mostly βgal-negative, whereas chains of βgal+/DCX+

neuroblasts left the dorsal wall/dorsolateral corner of the SVZ and entered the RMS side by side with βgal-negative neuroblasts. Interestingly, the differential distribution of βgal+/DCX+ neuroblasts versus βgal-negative/DCX+ neuroblasts recapitulates the heterogeneous origin of the SVZ from embryonic cerebral cortex and lateral ganglionic eminence, respectively (Young et al., 2007).

While Calbindin+ neurons in the OB of mGFAP/Ptet-Cre/R26R mice consistently lacked βgal immunoreactivity, two other major classes of GABAergic interneurons (Kohwi et al., 2007; Panzanelli et al., 2007) showed βgal expression, namely Calretinin+ and TH+ neurons. Cells derived from the embryonic cortex have been shown to settle in the dorsal aspects of the SVZ as well as in the RMS and to contribute new Calretinin+ and TH+ interneurons to the adult OB (Merkle et al., 2007; Young et al., 2007). Furthermore, studies using adenoviral or transgenic stem cell labeling in the SVZ found that adult Calbindin+ neurons are derived from the lateral wall of the SVZ (Merkle et al., 2007; Young et al., 2007). Taken together, the selective targeting of GFAP+ cells in the dorsal/dorsolateral wall of the SVZ and in the RMS of our mGFAP-tTA mice leads to the generation of Calretinin+/βgal+, TH+/βgal+, but not of Calbindin+/βgal+ interneurons in the GL, which strongly suggests that these transgenic mice target and fate map a restricted population of GFAP+ progenitor cell derived from the embryonic cortex. It should be noted, however, that reporter-labeled Calbindin+ interneurons were also not detected in GLAST-CreERT2/R26R fate-mapping mice, although these mice target both the dorsal and lateral walls of the SVZ (Ninkovic et al., 2007).

Reporter protein expression outside the established neurogenic regions (SGZ and SVZ) was restricted to GFAP+ astrocytes. Ptet-controlled expression of the reporter was primarily noted in the vicinity of the lateral ventricles including the entire roof and posterior wall of the lateral ventricle, but sparing its lateral wall. Reporter protein expression also followed remnant embryonic ventricular structures such as the subcallosal zone and the hippocampal and rhinal fissures. Intriguingly, neural stem cells residing in the subcallosal zone and in the posterior wall of the lateral ventricle have recently been described (Seaberg and van der Kooy, 2002; Seri et al., 2006).

Other brain regions which contain targeted astrocytes include the white cerebellar matter, corpus callosum, and fimbria hippocampi. The relative selectivity of the mGFAP-tTA line for GFAP+ progenitor cells in the adult neurogenic zones will be advantageous for studies which aim to target candidate gene overexpression to either GFAP+ progenitors of the SGZ or of the dorsal wall/dorsolateral corner of the lateral ventricles.

Taken together, despite being exclusively glia-specific, our mGFAP-tTA mouse line does not show the expected uniform targeting of all GFAP+ cells, but displays expression only in a subset of GFAP+ astrocytes, including all GFAP+ progenitor cells of the SGZ and a subset of GFAP+ progenitor cells residing in the dorsal wall/dorsolateral corner of the SVZ. This apparent restriction to a subset of GFAP+ astrocytes may either be caused by an integration effect of the plasmid-derived transgene (Bronson et al., 1996; Chandler et al., 2007; Wallace et al., 2000) or, alternatively, by the short regulatory sequences in the 2 kb murine GFAP promoter fragment driving tTA expression in our system.

Reliable Ptet-Controlled Target Gene Expression in GFAP+ Progenitor Cells

In the tet-system, inducible overexpression of target genes depends on the expression level of the transactivator tTA as well as on the accessibility of Ptet-response constructs at their genomic integration site (Schönig and Bujard, 2003). Activation and suppression of Ptet-controlled gene expression is regulated by Dox treatment which further complicates matters as Ptet-controlled gene expression has to be silent in the presence of Dox but activatable after Dox withdrawal.

Using four tet-regulated transgenes (Ptet-nLacZ, Ptet-EGFP, Ptet-Cre/R26R, Ptet-DTA), we here demonstrate the suitability of mGFAP-tTA mice to reliably and inducibly direct Ptet-controlled gene expression to GFAP+ progenitor cells of the DG and dorsal wall/dorsolateral corner of the lateral ventricles.

In the DG, regardless of the Ptet transgene, all double transgenic tTAxPtet mice displayed strong Ptet-controlled transgene expression in the absence of Dox. In fact, even in quadruple-transgenic mGFAP-tTA/Ptet-DTA/Ptet-Cre/R26R mice, Ptet-controlled gene expression was faithfully reproduced from two independent tet-promoters (Ptet-Cre and Ptet-DTA). Thus, strong cell-type specific tTA expression renders it possible to combine inducible gene expression with lineage tracing.

In the SVZ, the complexity of the conditional tet-system becomes evident. While Ptet-controlled gene expression of three different transgenes (Ptet-nLacZ, Ptet-EGFP, Ptet-Cre/R26R) was observed in the dorsal wall/dorsolateral corner of the lateral ventricles, we did not detect Ptet-controlled DTA expression in this region. Hence, despite adequate GFAP-promoter driven tTA expression in the dorsal wall/dorsolateral corner, Ptet-controlled DTA expression could not be achieved. Ptet-DTA transgenic mice, like all investigated Ptet-response lines, were generated via pronuclear injection of plasmid-derived DNA, which results in random integration of the transgene into the genome. The integration site may exert a profound effect on expression of the transgene (Chandler et al., 2007; Wallace et al., 2000; Weber et al., 2009), in particular when short DNA sequences (plasmid-derived) (Chandler et al., 2007) and inducible systems (tet-system) are used (Schönig and Bujard, 2003). Taken together, the restricted pattern of DTA expression argues for a positional integration effect of the Ptet-DTA transgene.

Simultaneous Target Gene Expression in GFAP+ Progenitor Cells and Fate Mapping of Their Progeny

To date, candidate genes influencing adult neurogenesis have been investigated primarily by inducible knock-

out models using the CreERT/loxP system. For this purpose, different promoters such as GLAST, hGFAP, Fgfr3, or nestin, have been utilized to control CreERT-expression (Balordi and Fishell, 2007; Breunig et al., 2007; Colak et al., 2008; Kuo et al., 2006; Young et al., 2010). Only recently, inducible gene deletion has been combined with an EGFP reporter for additional lineage tracing (Gao et al., 2009; Lagace et al., 2008). Conversely, only few studies have investigated the effects of inducible target gene overexpression on adult neurogenesis (Dupret et al., 2008; Farioli-Vecchioli et al., 2008). These studies used nestin-rtTA mice (Mitsuhashi et al., 2001) which allow overexpression of Ptet-controlled candidate genes in progenitor cells of the adult DG but not in the SVZ (Dupret et al., 2008). As compared with the GFAP promoter, the nestin promoter has the advantage of being spatially restricted to areas of constitutive neurogenesis in the adult murine brain. However, in the DG, the nestin promoter is active in phenotypically diverse progenitor cell populations (Fukuda et al., 2003). Therefore, the exact population of progenitor cells targeted as well as targeting efficiency remains to be further examined in nestin-rtTA mice (Dupret et al., 2008; Farioli-Vecchioli et al., 2008). From the available data, it can be inferred that the nestin-rtTA line targets a fraction of both astrocyte-like stem cells (type-1 cells) as well as transient intermediate progenitors (type-2 cells) in the DG of adult mice (Dupret et al., 2008). By contrast, the mGFAP-tTA line described here selectively targets virtually all type-1 cells in the DG and a subset of type-1 cells in the dorsal wall/dorsolateral corner of the SVZ. Furthermore, the above mentioned studies had to rely on BrdU-labeling protocols to assess the acute and long-term effects of genetic manipulation in nestin+ cells (Dupret et al., 2008; Farioli-Vecchioli et al., 2008) whereas our system allows target gene expression in GFAP+ type-1 cells in conjunction with βgal-assisted fate mapping. The high targeting efficiency of GFAP+ type-1 cells in the DG as verified in double-transgenic mGFAP-tTA/Ptet-DTA mice distinguishes the mGFAP-tTA line from other inducible transgenic mouse lines targeting adult neurogenesis (Beech et al., 2004; Breunig et al., 2007; Casper et al., 2007; Lagace et al., 2007; Mitsuhashi et al., 2001; Yu et al., 2005).

To our knowledge, this is the first report to introduce a multimodal system which permits inducible expression of a candidate gene in GFAP+ neural progenitors along with lineage tracing with a reporter protein. Triple-transgenic mGFAP-tTA/Ptet-Cre/R26R fate-mapping mice may be particularly useful to study the effects of environmental or pharmacological interventions on GFAP+ type-1 cells and their progeny. Quadruple-transgenic mice will enable researchers to precisely delineate the effects of candidate gene expression in GFAP+ type-1 cells on the entire process of adult neurogenesis. Notably, the breeding of quadruple-transgenic offspring from homozygous Ptet-Cre/R26R mice at the level of double-transgenic crossings makes this system practical and permits the generation of a sufficient number of quadruple-transgenic offspring. The examples given here highlight the great potential of our mGFAP-tTA mouse line for both fate mapping as well as functional manipulation of neurogenesis.

REFERENCES

Alonso M, Ortega-Perez I, Grubb MS, Bourgeois JP, Charneau P, Lledo PM. 2008. Turning astrocytes from the rostral migratory stream into neurons: A role for the olfactory sensory organ. J Neurosci 28:11089–11102.

Alvarez-Buylla A, Seri B, Doetsch F. 2002. Identification of neural stem cells in the adult vertebrate brain. Brain Res Bull 57:751–758.

Balordi F, Fishell G. 2007. Mosaic removal of hedgehog signaling in the adult SVZ reveals that the residual wild-type stem cells have a limited capacity for self-renewal. J Neurosci 27:14248–14259.

Beech RD, Cleary MA, Treloar HB, Eisch AJ, Harrist AV, Zhong W, Greer CA, Duman RS, Picciotto MR. 2004. Nestin promoter/enhancer directs transgene expression to precursors of adult generated periglomerular neurons. J Comp Neurol 475:128–141.

Breunig JJ, Silbereis J, Vaccarino FM, Sestan N, Rakic P. 2007. Notch regulates cell fate and dendrite morphology of newborn neurons in the postnatal dentate gyrus. Proc Natl Acad Sci USA 104: 20558–20563.

Bronson SK, Plaehn EG, Kluckman KD, Hagaman JR, Maeda N, Smithies O. 1996. Single-copy transgenic mice with chosen-site integration. Proc Natl Acad Sci USA 93:9067–9072.

Carleton A, Petreanu LT, Lansford R, Alvarez-Buylla A, Lledo PM. 2003. Becoming a new neuron in the adult olfactory bulb. Nat Neurosci 6:507–518.

Casper KB, Jones K, McCarthy KD. 2007. Characterization of astrocyte-specific conditional knockouts. Genesis 45:292–299.

Chandler KJ, Chandler RL, Broeckelmann EM, Hou Y, Southard-Smith EM, Mortlock DP. 2007. Relevance of BAC transgene copy number in mice: Transgene copy number variation across multiple transgenic lines and correlations with transgene integrity and expression. Mamm Genome 18:693–708.

Colak D, Mori T, Brill MS, Pfeifer A, Falk S, Deng C, Monteiro R, Mummery C, Sommer L, Gotz M. 2008. Adult neurogenesis requires Smad4-mediated bone morphogenic protein signaling in stem cells. J Neurosci 28:434–446.

Delaney CL, Brenner M, Messing A. 1996. Conditional ablation of cerebellar astrocytes in postnatal transgenic mice. J Neurosci 16:6908–6918.

Doetsch F. 2003. The glial identity of neural stem cells. Nat Neurosci 6:1127–1134.

Doetsch F, Caille I, Lim DA, Garcia-Verdugo JM, Alvarez-Buylla A. 1999. Subventricular zone astrocytes are neural stem cells in the adult mammalian brain. Cell 97:703–716.

Dupret D, Revest JM, Koehl M, Ichas F, De Giorgi F, Costet P, Abrous DN, Piazza PV. 2008. Spatial relational memory requires hippocampal adult neurogenesis. PLoS ONE 3:e1959.

Farioli-Vecchioli S, Saraulli D, Costanzi M, Pacioni S, Cina I, Aceti M, Micheli L, Bacci A, Cestari V, Tirone F. 2008. The timing of differentiation of adult hippocampal neurons is crucial for spatial memory. PLoS Biol 6:e246.

Filippov V, Kronenberg G, Pivneva T, Reuter K, Steiner B, Wang LP, Yamaguchi M, Kettenmann H, Kempermann G. 2003. Subpopulation of nestin-expressing progenitor cells in the adult murine hippocampus shows electrophysiological and morphological characteristics of astrocytes. Mol Cell Neurosci 23:373–382.

Fukuda S, Kato F, Tozuka Y, Yamaguchi M, Miyamoto Y, Hisatsune T. 2003. Two distinct subpopulations of nestin-positive cells in adult mouse dentate gyrus. J Neurosci 23:9357–9366.

Gao Z, Ure K, Ables JL, Lagace DC, Nave KA, Goebbels S, Eisch AJ, Hsieh J. 2009. Neurod1 is essential for the survival and maturation of adult-born neurons. Nat Neurosci 12:1090–1092.

Garcia AD, Doan NB, Imura T, Bush TG, Sofroniew MV. 2004. GFAP-expressing progenitors are the principal source of constitutive neurogenesis in adult mouse forebrain. Nat Neurosci 7:1233–1241.

Gregorian C, Nakashima J, Le Belle J, Ohab J, Kim R, Liu A, Smith KB, Groszer M, Garcia AD, Sofroniew MV, Carmichael ST, Kornblum HI, Liu X, Wu H. 2009. Pten deletion in adult neural stem/progenitor cells enhances constitutive neurogenesis. J Neurosci 29:1874–1886.

Gritti A, Bonfanti L, Doetsch F, Caille I, Alvarez-Buylla A, Lim DA, Galli R, Verdugo JM, Herrera DG, Vescovi AL. 2002. Multipotent neural stem cells reside into the rostral extension and olfactory bulb of adult rodents. J Neurosci 22:437–445.

Imayoshi I, Sakamoto M, Ohtsuka T, Takao K, Miyakawa T, Yamaguchi M, Mori K, Ikeda T, Itohara S, Kageyama R. 2008. Roles of continuous neurogenesis in the structural and functional integrity of the adult forebrain. Nat Neurosci 11:1153–1161.

Imura T, Kornblum HI, Sofroniew MV. 2003. The predominant neural stem cell isolated from postnatal and adult forebrain but not early embryonic forebrain expresses GFAP. J Neurosci 23:2824–2832.

Johnson WB, Ruppe MD, Rockenstein EM, Price J, Sarthy VP, Verderber LC, Mucke L. 1995. Indicator expression directed by regulatory sequences of the glial fibrillary acidic protein (GFAP) gene: In vivo comparison of distinct GFAP-lacZ transgenes. Glia 13:174–184.

Kempermann G, Gast D, Kronenberg G, Yamaguchi M, Gage FH. 2003. Early determination and long-term persistence of adult-generated new neurons in the hippocampus of mice. Development 130:391–399.

Kempermann G, Jessberger S, Steiner B, Kronenberg G. 2004. Milestones of neuronal development in the adult hippocampus. Trends Neurosci 27:447–452.

Kistner A, Gossen M, Zimmermann F, Jerecic J, Ullmer C, Lubbert H, Bujard H. 1996. Doxycycline-mediated quantitative and tissue-specific control of gene expression in transgenic mice. Proc Natl Acad Sci USA 93:10933–10938.

Kohwi M, Petryniak MA, Long JE, Ekker M, Obata K, Yanagawa Y, Rubenstein JL, Alvarez-Buylla A. 2007. A subpopulation of olfactory bulb GABAergic interneurons is derived from Emx1- and Dlx5/6-expressing progenitors. J Neurosci 27:6878–6891.

Kronenberg G, Reuter K, Steiner B, Brandt MD, Jessberger S, Yamaguchi M, Kempermann G. 2003. Subpopulations of proliferating cells of the adult hippocampus respond differently to physiologic neurogenic stimuli. J Comp Neurol 467:455–463.

Kuan CY, Schloemer AJ, Lu A, Burns KA, Weng WL, Williams MT, Strauss KI, Vorhees CV, Flavell RA, Davis RJ, Sharp FR, Rakic P. 2004. Hypoxia-ischemia induces DNA synthesis without cell proliferation in dying neurons in adult rodent brain. J Neurosci 24:10763–10772.

Kuo CT, Mirzadeh Z, Soriano-Navarro M, Rasin M, Wang D, Shen J, Sestan N, Garcia-Verdugo J, Alvarez-Buylla A, Jan LY, Jan YN. 2006. Postnatal deletion of Numb/Numblike reveals repair and remodeling capacity in the subventricular neurogenic niche. Cell 127:1253–1264.

Lagace DC, Benavides DR, Kansy JW, Mapelli M, Greengard P, Bibb JA, Eisch AJ. 2008. Cdk5 is essential for adult hippocampal neurogenesis. Proc Natl Acad Sci USA 105:18567–18571.

Lagace DC, Whitman MC, Noonan MA, Ables JL, DeCarolis NA, Arguello AA, Donovan MH, Fischer SJ, Farnbauch LA, Beech RD, DiLeone RJ, Greer CA, Mandyam CD, Eisch AJ. 2007. Dynamic contribution of nestin-expressing stem cells to adult neurogenesis. J Neurosci 27:12623–12629.

Maxwell F, Maxwell IH, Glode LM. 1987. Cloning, sequence determination, and expression in transfected cells of the coding sequence for the tox 176 attenuated diphtheria toxin A chain. Mol Cell Biol 7:1576–1579.

Mayford M, Bach ME, Huang YY, Wang L, Hawkins RD, Kandel ER. 1996. Control of memory formation through regulated expression of a CaMKII transgene. Science 274:1678–1683.

Mendoza-Torreblanca JG, Martinez-Martinez E, Tapia-Rodriguez M, Ramirez-Hernandez R, Gutierrez-Ospina G. 2008. The rostral migratory stream is a neurogenic niche that predominantly engenders periglomerular cells: In vivo evidence in the adult rat brain. Neurosci Res 60:289–299.

Merkle FT, Mirzadeh Z, Alvarez-Buylla A. 2007. Mosaic organization of neural stem cells in the adult brain. Science 317:381–384.

Merkle FT, Tramontin AD, Garcia-Verdugo JM, Alvarez-Buylla A. 2004. Radial glia give rise to adult neural stem cells in the subventricular zone. Proc Natl Acad Sci USA 101:17528–17532.

Mitsuhashi T, Aoki Y, Eksioglu YZ, Takahashi T, Bhide PG, Reeves SA, Caviness VS Jr. 2001. Overexpression of p27Kip1 lengthens the G1 phase in a mouse model that targets inducible gene expression to central nervous system progenitor cells. Proc Natl Acad Sci USA 98:6435–6440.

Ninkovic J, Mori T, Gotz M. 2007. Distinct modes of neuron addition in adult mouse neurogenesis. J Neurosci 27:10906–10911.

Panzanelli P, Fritschy JM, Yanagawa Y, Obata K, Sassoe-Pognetto M. 2007. GABAergic phenotype of periglomerular cells in the rodent olfactory bulb. J Comp Neurol 502:990–1002.

Schönig K, Bujard H. 2003. Generating conditional mouse mutants via tetracycline controlled gene expression. In: van Deursen J, Hofker M, editors. Transgenic mouse: Methods and protocols. Totowa: Humana Press. pp 69–104.

Schönig K, Schwenk F, Rajewsky K, Bujard H. 2002. Stringent doxycycline dependent control of CRE recombinase in vivo. Nucleic Acids Res 30:e134

Seaberg RM, van der Kooy D. 2002. Adult rodent neurogenic regions: The ventricular subependyma contains neural stem cells, but the dentate gyrus contains restricted progenitors. J Neurosci 22: 1784–1793.

Seri B, Garcia-Verdugo JM, McEwen BS, Alvarez-Buylla A. 2001. Astrocytes give rise to new neurons in the adult mammalian hippocampus. J Neurosci 21:7153–7160.

Seri B, Herrera DG, Gritti A, Ferron S, Collado L, Vescovi A, Garcia-Verdugo JM, Alvarez-Buylla A. 2006. Composition and organization of the SCZ: A large germinal layer containing neural stem cells in the adult mammalian brain. Cereb Cortex 16(Suppl 1):i103–i111.

Soriano P. 1999. Generalized lacZ expression with the ROSA26 Cre reporter strain. Nat Genet 21:70–71.

Taupin P. 2007. BrdU immunohistochemistry for studying adult neurogenesis: Paradigms, pitfalls, limitations, and validation. Brain Res Rev 53:198–214.

Urlinger S, Baron U, Thellmann M, Hasan MT, Bujard H, Hillen W. 2000. Exploring the sequence space for tetracycline-dependent transcriptional activators: Novel mutations yield expanded range and sensitivity. Proc Natl Acad Sci USA 97:7963–7968.

Wallace H, Ansell R, Clark J, McWhir J. 2000. Pre-selection of integration sites imparts repeatable transgene expression. Nucleic Acids Res 28:1455–1464.

Weber T, Bohm G, Hermann E, Schutz G, Schonig K, Bartsch D. 2009. Inducible gene manipulations in serotonergic neurons. Front Mol Neurosci 2:24

Yamaizumi M, Mekada E, Uchida T, Okada Y. 1978. One molecule of diphtheria toxin fragment A introduced into a cell can kill the cell. Cell 15:245–250.

Young KM, Fogarty M, Kessaris N, Richardson WD. 2007. Subventricular zone stem cells are heterogeneous with respect to their embryonic origins and neurogenic fates in the adult olfactory bulb. J Neurosci 27:8286–8296.

Young KM, Mitsumori T, Pringle N, Grist M, Kessaris N, Richardson WD. 2010. An Fgfr3-iCreER(T2) transgenic mouse line for studies of neural stem cells and astrocytes. Glia 58:943–953.

Yu TS, Dandekar M, Monteggia LM, Parada LF, Kernie SG. 2005. Temporally regulated expression of Cre recombinase in neural stem cells. Genesis 41:147–153.